ELSEVIER

Biochimica et Biophysica Acta 1587 (2002) 118–125

BIOCHIMICA ET BIOPHYSICA ACTA
BBA

www.bba-direct.com

Review

A simple model to predict blood–brain barrier permeation from 3D molecular fields

Frédéric Ooms, Peter Weber, Pierre-Alain Carrupt, Bernard Testa*

Institut de Chimie Thérapeutique, Section de Pharmacie, BEP, Université de Lausanne, CH-1015 Lausanne, Switzerland

Received 6 September 2001; accepted 15 October 2001

Abstract

We report a four-component partial least squares discriminant analysis (PLS) model for the prediction of blood–brain barrier (BBB) permeation using descriptors derived from 3D molecular fields. The 3D fields were transformed by VolSurf into suitable 1D descriptors, which were correlated to the ratio of blood–brain partitioning measured at steady state in rats (log C_{brain}/C_{blood}). The model so obtained sheds light on molecular properties influencing BBB permeation. It can also be used in the virtual screening of new chemicals.

Keywords: Blood–brain barrier; Brain penetration; QSAR

1. Introduction

The blood–brain barrier (BBB) has peculiar characteristics among the various physiological barriers. Diffusion of drugs across this endothelium separating the blood from the central nervous system (CNS) is in fact more restrictive than elsewhere. Endothelial cells provide a crucial interface between blood and tissues. The free diffusion of chemicals across endothelia is prevented by endothelial tight junctions, the permeability of which varies considerably depending on tissue and conditions. In peripheral tissues (intestine, kidney, salivary gland), these cell barriers have fenestrations enabling relatively facile exchange of water and solutes. In contrast, the endothelial barrier separating the blood from the CNS is characterized by tight junctions of severely limited permeability (excluding molecules with a diameter larger than 20 Å), no fenestrae and an attenuated pinocytosis [1,2].

As a common feature, both peripheral and blood–brain endothelial cells have significant metabolic activity [3]. Moreover, and in contrast to what was for long the common view, the special features of the BBB seem to be subject to endogenous regulation [1].

Thus, the BBB is far from being a simple barrier. Understanding its structure and functions, as well as the physicochemical and biological factors that control solute transfer, is a problem of great currency in pharmaceutical research. This is true not only for the design and development of CNS-active agents, but also for drugs that must be forbidden entry into the CNS to avoid unwanted side-effects, as exemplified by anti-histamines [4] and β-blockers [5]. Hence, in drug discovery, early assessment of BBB permeation is of great importance, and in vitro and in vivo techniques have been devised for this purpose [6].

Besides these experimental techniques, computational approaches have also been developed to predict the BBB permeation of new chemicals since the experimental determination of BBB penetration is laborious, expensive, time-consuming and requires a sufficient quantity of pure compound, often in radiolabeled form, to obtain good experimental data. Therefore, a fast and reliable computational method to predict BBB permeation at an early stage of discovery could help decrease the attrition curve since it would allow the virtual screening of many compounds prior to synthesis. Over the years, various authors have attempted to predict BBB transport using lipophilicity (log *P*) [7–9], solvatochromic parameters [10], H-bonding capacity [11–14], topolog-

Abbreviations: BBB, blood–brain barrier; CNS, central nervous system; MIF, molecular interaction field; PCA, principal component analysis; PLS, partial least squares discriminant analysis; PSA, polar surface area

* Corresponding author. Tel.: +41-21-692-4521; fax: +41-21-692-4525.
E-mail address: Bernard.Testa@ict.unil.ch (B. Testa).

0925-4439/02/$ - see front matter
PII: S0925-4439(02)00074-1

ical indices [15], polar surface area (PSA) [16–19] and Molsurf descriptors [20].

Recently, a new method named VolSurf has been developed by Cruciani et al. [21]. This method is able to convert 3D fields into new descriptors well suited for structure–pharmacokinetic relationships [22,23] and have proven its efficacy, simplicity of use and chemical interpretability (see Ref. [21] for a detailed description of the method). A previous semiquantitative model was able to classify correctly more than 90% of BBB+ and BBB − permeation data [23]. In the present work, a quantitative model is presented, which was derived from log(C_{brain}/C_{blood}) steady-state (log BB) values of 83 compounds measured in rats.

2. Experimental procedures

2.1. Overview

The overall procedure consisted in the following four major steps:

1. Compilation of a homogenous set of literature BBB data for 83 compounds.
2. Calculation of their 3D structure.
3. Computation of their molecular interaction fields (MIFs) using GRID probes.
4. Generation of the VolSurf descriptors.

Table 1
Experimental and calculated log BB values for the compounds included in this study

Compound	Name	log BB_{exp}	log BB_{calc}	Reference	Compound	Name	log BB_{exp}	log BB_{calc}	Reference
1	cimetidine	− 1.42	− 1.188	[14]	**44**	valproic-acid	− 0.22	0.598	[25]
2	clonidine	0.11	0.462	[14]	**45**	chlorambucil	− 1.70	outlier	[15]
3		− 0.04	− 0.563	[14]	**46**		− 1.3	− 1.162	[11]
4	imipramine	0.83	0.923	[14]	**47**		− 1.4	− 0.918	[11]
5	mepyramine	0.49	0.521	[14]	**48**		− 0.43	− 0.397	[15]
6	ranitidine	− 1.23	− 0.605	[14]	**49**		0.25	0.193	[15]
7	tiotidine	− 0.82	− 1.144	[14]	**50**		− 0.3	− 0.244	[11]
8	icotidine	− 2	− 1.222	[14]	**51**		− 0.06	0.468	[11]
9	SKF-93619	− 1.3	− 0.410	[14]	**52**		− 0.42	− 1.435	[11]
10	lupitidine	− 1.06	− 1.232	[14]	**53**		− 0.16	0.222	[15]
11		− 1.17	− 0.707	[14]	**54**	thioridazine	0.24	0.781	[25]
12		− 2.15	outlier	[14]	**55**	chlorpromazine	1.06	0.422	[25]
13		− 0.67	− 0.718	[14]	**56**	desipramine	1.2	0.420	[25]
14		− 0.66	− 0.680	[14]	**57**	alprazolam	0.044	− 0.375	[25]
15		− 0.12	− 0.603	[14]	**58**	codeine	0.55	0.543	[25]
16		− 0.18	− 0.282	[14]	**59**	didanosine	− 1.301	− 1.296	[15]
17		− 1.15	− 0.669	[14]	**60**	oxazepam	0.61	− 0.659	[25]
18		− 1.57	− 1.313	[14]	**61**	verapamil	− 0.7	− 0.960	[25]
19		− 1.54	− 1.252	[14]	**62**	trifluopromazine	1.44	outlier	[25]
20		− 1.12	− 0.739	[14]	**63**	theophylline	− 0.29	− 0.955	[25]
21		− 0.73	− 0.763	[14]	**64**	pentobarbital	0.12	− 0.535	[25]
22		− 0.27	− 0.231	[14]	**65**	hyroxyzine	0.39	− 0.881	[25]
23		− 0.28	− 0.492	[14]	**66**	midazolam	0.36	0.412	[25]
24		− 0.46	0.158	[14]	**67**	promazine	1.23	0.651	[25]
25		− 0.24	0.111	[14]	**68**	physostigmine	0.079	0.380	[15]
26		− 0.02	− 0.037	[14]	**69**	nevirapine	0	0.083	[15]
27		0.69	0.322	[14]	**70**	mianserin	0.99	0.906	[17]
28		0.44	− 0.222	[14]	**71**	Org-4428	0.82	1.010	[17]
29	zolantidine	0.14	− 0.277	[14]	**72**	Org-5222	1.03	0.614	[17]
30		0.22	0.186	[14]	**73**	Org-12962	1.64	outlier	[17]
31	amitriptyline	0.89	0.742	[10]	**74**	Org-32104	0.52	0.066	[17]
32	carbamazepine	0	0.313	[15]	**75**	Org-30526	0.39	0.036	[17]
33		− 0.34	− 0.153	[15]	**76**	mirtazapine	0.53	0.506	[17]
34	L-663581	− 0.3	− 0.089	[24]	**77**	tibolone	0.4	0.911	[17]
35	M1L-663581	− 1.34	− 0.882	[24]	**78**	domperidone	− 0.78	− 0.586	[17]
36	M2L-663581	− 1.82	− 1.568	[24]	**79**	Org-34167	0	0.240	[17]
37	antipyrine	− 0.097	0.495	[25]	**80**	risperidone	− 0.02	− 0.479	[17]
38	caffeine	− 0.055	− 0.870	[25]	**81**	9-OH-risperidone	− 0.67	− 0.909	[17]
39	ibuprofen	− 0.18	0.220	[25]	**82**	BCNU	− 0.52	− 0.191	[15]
40	indomethacin	− 1.26	− 1.146	[25]	**83**	phenserine	1	0.679	[15]
41	salicylic-acid	− 1.1	− 0.657	[25]					
42	temelastine	− 1.88	− 1.059	[26]					
43	aspirin	− 0.5	− 0.516	[25]					

5. Statistical analysis using principal component analysis (PCA) and partial least squares discriminant analysis (PLS).

Steps 3–5 were performed automatically by the VolSurf program.

2.2. Dataset

Log BB data for 83 radiolabeled compounds were compiled from the literature (Table 1) [10,11,14,15,17,24–26]. These values were blood/brain concentration ratios obtained in the rat at steady state:

$$\log BB = \log(C_{brain}/C_{blood}) \quad (1)$$

The values within this dataset ranged from −2.16 to 1.64. A basic assumption of the study was that BBB permeation was purely passive.

2.3. Modelling of 3D molecular structures

The 3D structure of the selected compounds (Fig. 1) were drawn starting from the Corina-built structures, and energy-optimized using the MMFF94s force field including MMFF94 partial atomic charges as implemented in Sybyl 6.4 [27]. Minimization was performed in vacuo ($\varepsilon = 1$) using BFGS and continued until the root-mean-square energy gradient was lower than 0.001 kcal/mol. All molecules were built in their neutral forms. Because it is impossible to model mixtures of stereoisomers in 3D and since VolSurf descriptors are achiral, only one of stereoisomer was modelled.

2.4. Calculation of VolSurf descriptors and statistical analysis

The MIFs were calculated using the water, DRY, and carbonyl probes available in the GRID program [28]. The GRID forcefield is indeed well suited to characterize putative polar and hydrophobic interaction sites around target molecules. The water probe was used to simulate hydration–dehydration processes, the hydrophobic (DRY) probe was used to simulate drug–membrane hydrophobic interactions, and the carbonyl probe was used to simulate drug–membrane H-bonding interactions [23]. Descriptors were then automatically generated by VolSurf. These descriptors refer to molecular size and shape, to size and shape of hydrophilic and hydrophobic regions, and to the balance between them. Hydrogen bonding, amphiphilic moments

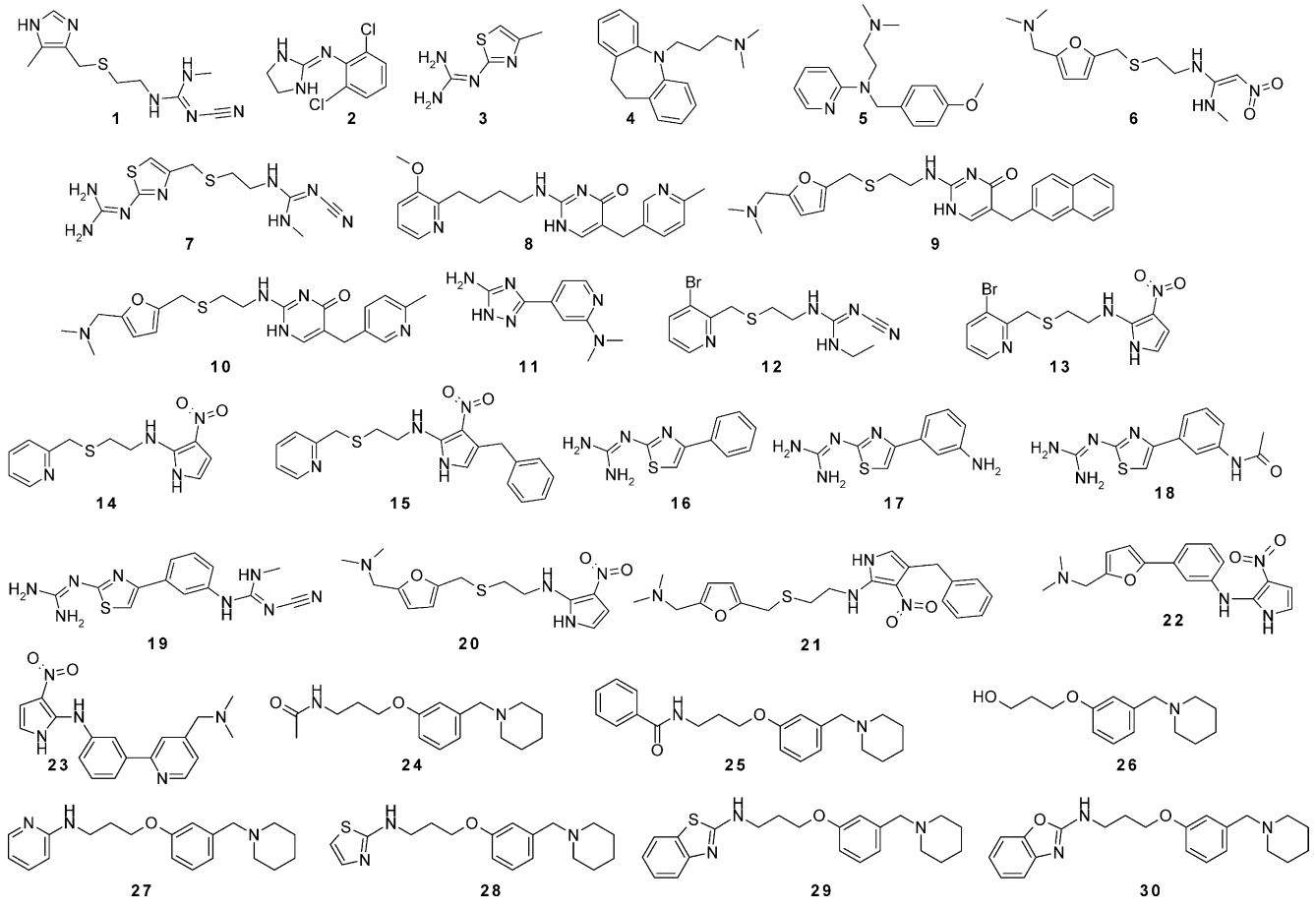

Fig. 1. Chemical structure of the compounds in the dataset.

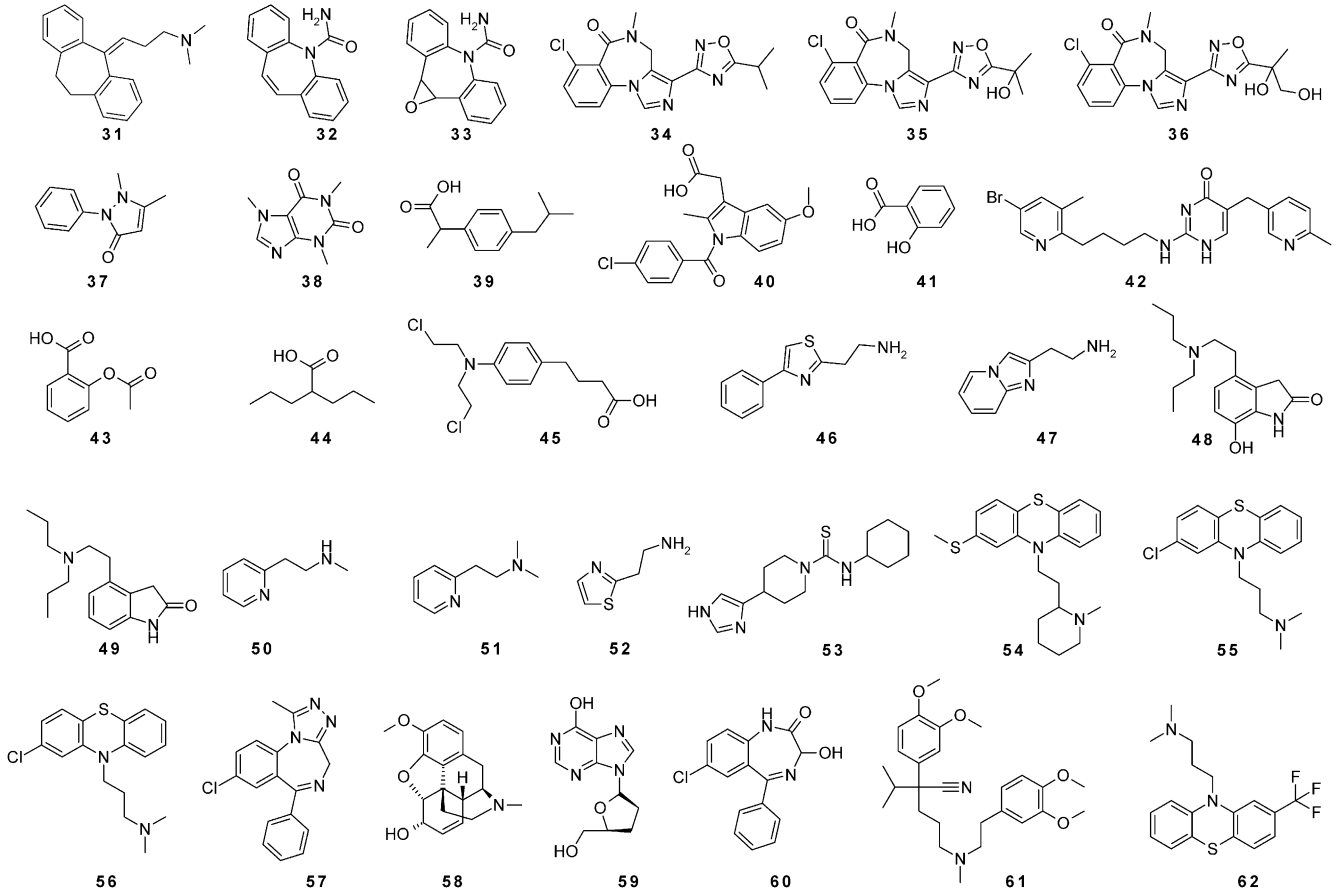

Fig. 1 (*continued*).

and critical packing parameters are other useful descriptors (for a more detailed description, see Ref. [21]).

PCA and PLS analyses were produced with the VolSurf program version 2.0.6. The number of significant latent variables and the quality of the models were determined using a leave-one-out cross-validation procedure (LOO-cv). In such a procedure, each compound is removed once from the dataset, and the remaining compounds are used to develop a new model, with which the left-out compound is then predicted.

3. Results and discussion

3.1. Preliminary BBB permeation model

In a first investigation, VolSurf molecular descriptors were computed for the 83 compounds included within the dataset using the water, DRY and carbonyl probes, yielding 72 descriptors. This led for the 83 compounds to a four-component PLS model (Table 2; model 1), which explained about 65% of the total variance of the matrix. The predictive ability of the model was assessed by means of cross-validation (leave-one-out). A detailed inspection of the predicted residual plots showed several strong outliers (eight compounds). Removing compounds **12** and **45** (the same outliers as in previous studies [10,15,26] and compounds **62** and **73** resulted for the 79 remaining compounds in an improved four-component PLS model (Table 2, model 1b). Compounds **62** and **73** were remove since a careful inspection of the MIFs obtained with the DRY probe showed that the trifluoromethyl group was not well described by this probe.

3.2. Final BBB permeation model and its interpretation

A systematic examination showed that it was possible to use only the three lowest energy levels calculated with the water and DRY probes, and canceling the carbonyl probe. Indeed, the correlation matrix revealed that several descriptors generated from the carbonyl probe correlated with those obtained with the water probe. This observation is not too surprising since the water probe already accounts for the polarity of the studied compounds.

As a result of these restrictions, the independent variables were reduced to 31 descriptors. The statistics of this new four-component PLS model (Table 2, model 2; Fig. 2) were similar to those of model 1b. The coefficient plot of this final model (Fig. 3) shows the contribution of the 31 VolSurf descriptors. The vertical bars represent the contri-

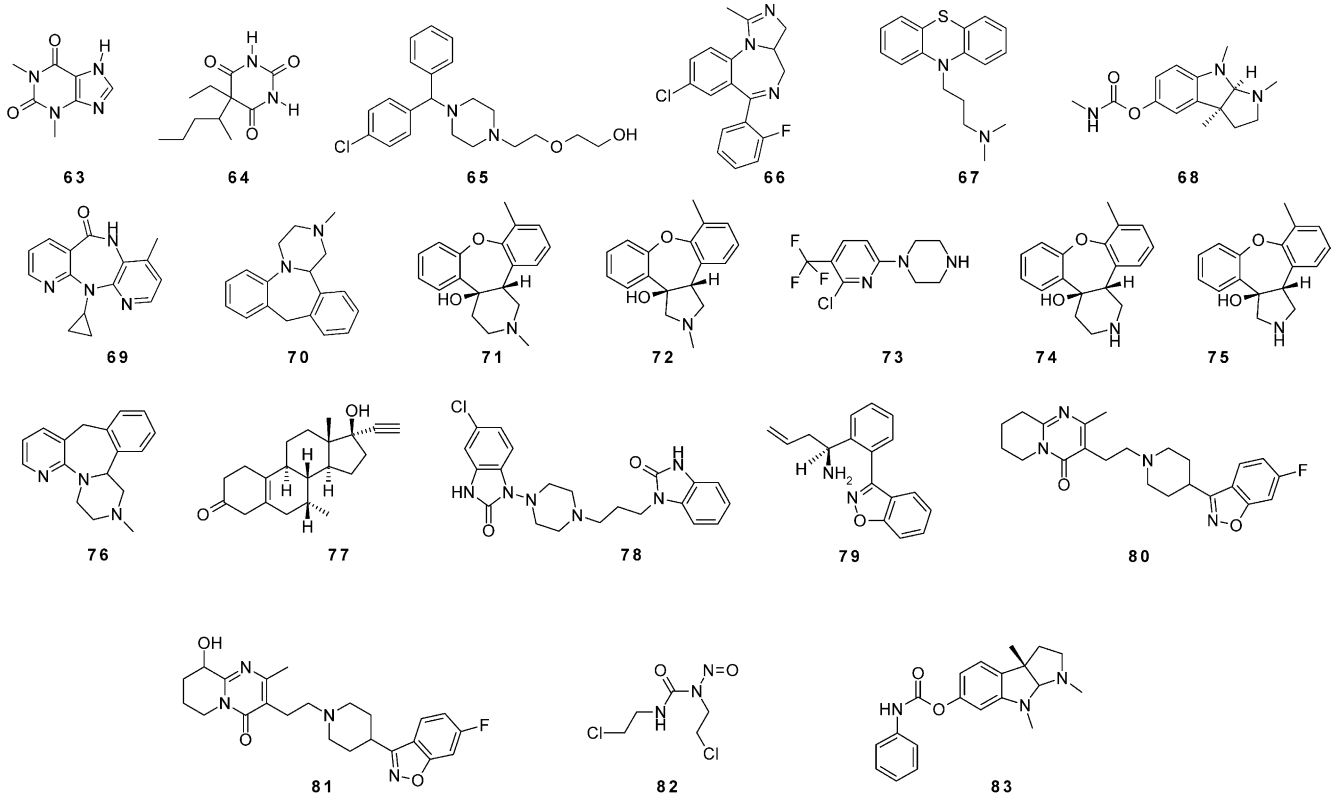

Fig. 1 (*continued*).

bution of each single descriptor, a short bar denoting a minor contribution and a long bar a major one. The last bar on the right represents the dependent variable, i.e. log BB. The following conclusions can be drawn from this plot:

- Descriptors of polarity such as hydrophilic regions (W1–W3) and capacity factors (CW1–CW3) are inversely correlated with BBB permeability. Their negative coefficients are in line with the well-known fact that highly polar compounds have a very low BBB permeation.
- The descriptors of hydrophobic interactions (D1–D3) are directly correlated with BBB permeation, although their positive contribution appears somewhat smaller than the negative contribution of the polar descriptors. These positive contributions are in accordance with the fact that lipophilic compounds penetrate relatively easily into the brain.
- The size and shape descriptors have no marked impact on BBB permeation except for rugosity, which correlates positively with BBB permeation, and globularity, which correlates negatively. Rugosity is defined as the ratio of total volume (V_{tot}) over total surface (S_{tot}), and it is smaller the more the object differs from a sphere. Globularity is defined as the ratio between S_{tot} and the surface of a sphere of equivalent volume (V_{tot}), and it is larger the more the object differs from a sphere. In other words, both descriptors indicate that compounds having a high rugosity and a low globularity will have a spherical shape and will be better at crossing the BBB.

Table 2
Statistical properties of the models

Model	Training set	*N* descriptors	r^2 (four LVs)	q^2
1	83 compounds	72	0.68	0.50
1b	79 compounds	72	0.78	0.65
2	79 compounds	31	0.76	0.65

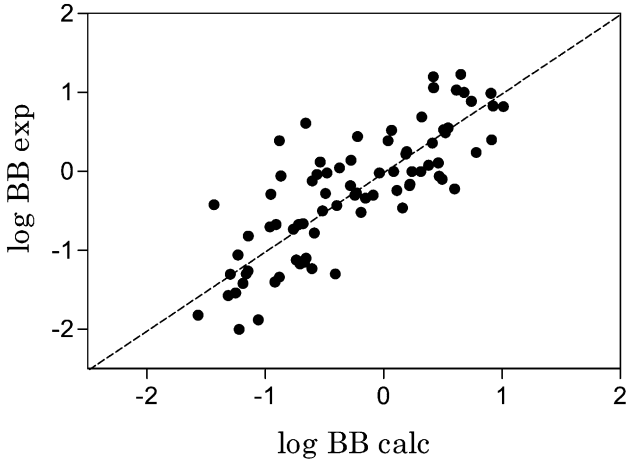

Fig. 2. Relationship between experimental and calculated BBB permeation using the four-component PLS model (Table 2, model 2).

3.3. Application to two compounds in the dataset

Here, we discuss in some detail two compounds to exemplify the interpretative value of the VolSurf model. These compounds are characterized by different BBB permeation properties: **70** easily crosses the BBB while **59** does not.

The scaled values of the descriptors (Fig. 4) show several trends:

- The hydrophilic descriptors (W1–W3, CW1–CW3) of **70** are lower than those of **59**.
- The hydrophobic descriptors (D1–D3) of **70** are larger than those of **59**.
- Relative to **59**, the rugosity of **70** is higher whereas the globularity is lower.

A visual comparison of the MIFs calculated around compounds **59** and **70** with the water and DRY probes also shows several differences (Fig. 5). The dark gray zones represent the hydrophilic regions in Fig. 5 left, and the hydrophobic regions in Fig. 5 right. As can be seen, the hydrophilic regions generated around **59** are larger than those around **70** while the reverse holds for the hydrophobic regions. These results are in agreement with our above analysis of the PLS coefficient plot (Fig. 3), namely that the size of the hydrophilic regions is inversely correlated with BBB permeation whereas the opposite is true for the hydrophobic regions. Furthermore, **70** indeed has a more spherical shape than **59**.

3.4. Interest of the model in virtual screening of BBB permeation

The four-component PLS model can also be used to perform a semiquantitative classification of compounds based on their permeation or nonpermeation of the BBB. Compounds having a log BB value >0 were classified has brain penetrators (BBB+) while those with a log BB value <0 were considered as not reaching the brain in sufficient concentrations (BBB−). It is important to note that this cutoff is arbitrary and would have to be defined with a specific pharmacology in mind. Indeed, the cutoff value will depend on which are more damaging to the classification, false positives or false negatives. Eighty-five percent of the BBB− compounds and 79% of BBB+ compounds were correctly classified with a cutoff of 0. If more restrictive cutoffs are chosen to define BBB− compounds (log BB <-0.5) and BBB+ compounds (log BB>0.5), the model correctly assign more than 90% of the BBB− compounds and 65% of the BBB+ compounds.

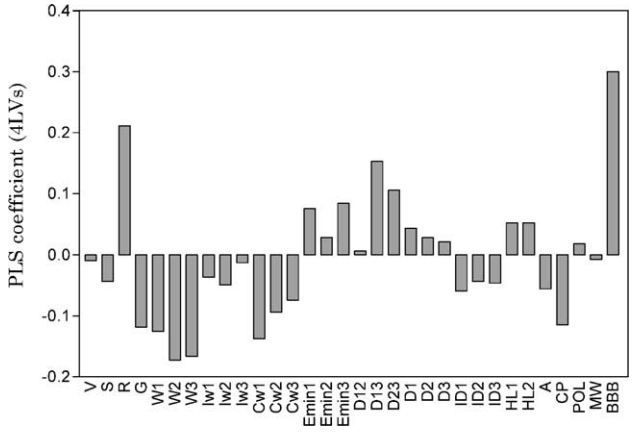

Fig. 3. PLS coefficient plot for the final model (Table 2, model 2) for the correlation of VolSurf descriptors with BBB permeation.

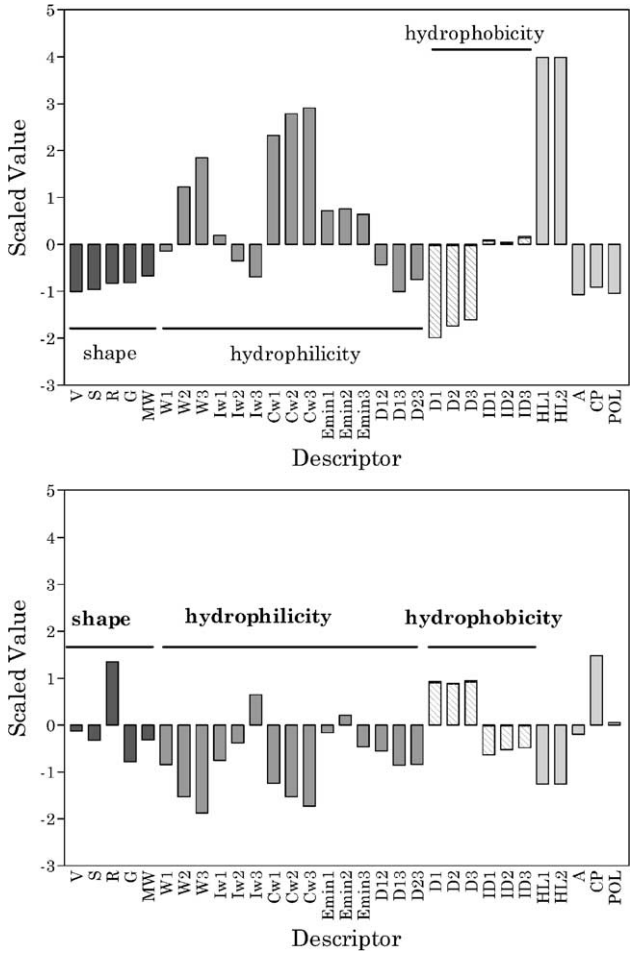

Fig. 4. Thirty-one VolSurf scaled descriptors calculated for compounds **59** (didanosine, upper part) and **70** (mianserine, lower part).

4. Conclusion

The model obtained in this study for the prediction of BBB permeation is relevant from a physiological point of view and is also in agreement with insights from other BBB permeation models. We show that VolSurf descriptors describing hydrophilic and hydrophobic properties are well

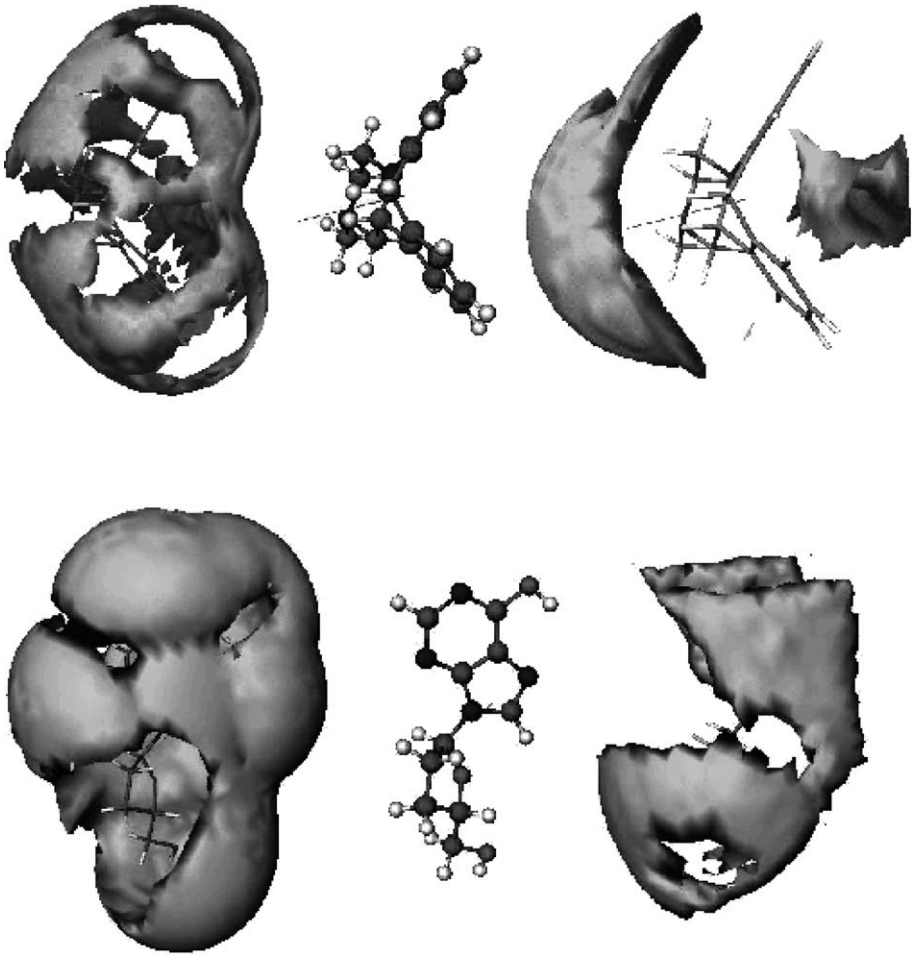

Fig. 5. GRID 3D molecular interaction fields of **70** (upper part) and **59** (lower part) calculated with the water (right) and the DRY (left) probes. The zones shown are contoured at −1 kcal/mol.

suited to derive a PLS model able to discriminate good and poor BBB penetrators. Finally, we believe that a more robust model to predict log BB values could be obtained from BBB data measured by a single experimental protocol and for compounds permeating by a purely passive mechanism.

Acknowledgements

The authors are indebted to Dr. Gabriele Cruciani for his interest and support.

References

[1] J.B.M.M. van Bree, A.G. de Boer, M. Danhof, D.D. Breimer, Drug transport across the blood–brain barrier: I. Anatomical and physiological aspects, Pharm. Weekbl., Sci. Ed. 14 (1992) 305–310.
[2] T. Hirase, J.M. Staddon, M. Saitou, Y. Ando-Akatsuka, M. Itoh, M. Furuse, K. Fujimoto, S. Tsukita, L.L. Rubin, Occludin as a possible determinant of tight junction permeability in endothelial cells, J. Cell Sci. 110 (1997) 1603–1613.
[3] M.W. Brightman, The anatomic basis of the blood–brain barrier, in: E.A. Neuwelt (Ed.), Implications of the Blood–Brain Barrier and Its Manipulation: Volume 1. Basic Science Aspects, Plenum, New York, 1989, pp. 53–83.
[4] A.M. ter Laak, R.S. Tsai, G.M. Donné-op den Kelder, P.A. Carrupt, B. Testa, H. Timmerman, Lipophilicity and hydrogen-bonding capacity of H1-antihistaminic agents in relation to their central sedative side-effects, Eur. J. Pharm. Sci. 2 (1994) 373–384.
[5] P.B. Woods, M.L. Robinson, An investigation of the comparative liposolubilities of β-adrenoceptor blocking agents, J. Pharm. Pharmacol. 33 (1981) 172–173.
[6] A. Pagliara, M. Reist, S. Geinoz, P.A. Carrupt, B. Testa, Evaluation and prediction of drug permeation, J. Pharm. Pharmacol. 51 (1999) 1339–1357.
[7] C. Hansch, J.M. Clayton, Lipophilic character and biological activity of drugs: II. The parabolic case, J. Pharm. Sci. 62 (1973) 1–21.
[8] C. Hansch, J.P. Björkroth, A. Leo, Hydrophobicity and central nervous system agents: on the principle of minimal hydrophobicity in drug design, J. Pharm. Sci. 76 (1987) 663–687.
[9] D.D. Dischino, M.J. Welch, M.R. Kilbourn, M.E. Raichle, Relationship between lipophilicity and brain extraction of C-11-labeled radiopharmaceuticals, J. Nucl. Med. 24 (1983) 1030–1038.
[10] F. Lombardo, J.F. Blake, W.J. Curatolo, Computation of brain–blood partitioning of organic solutes via free energy calculations, J. Med. Chem. 39 (1996) 4750–4755.
[11] R.C. Young, C.R. Ganellin, R. Griffiths, R.C. Mitchell, M.E. Parsons, D. Saunders, N.E. Sore, An approach to the design of brain-penetrating histaminergic agonists, Eur. J. Med. Chem. 28 (1993) 201–211.

[12] E.G. Chikhale, K.Y. Ng, P.S. Burton, R.T. Borchardt, Hydrogen bonding potential as a determinant of the in vitro and in situ blood–brain barrier permeability of peptides, Pharm. Res. 11 (1994) 412–419.
[13] H. van de Waterbeemd, M. Kansy, Hydrogen-bonding capacity and brain penetration, Chimia 46 (1992) 299–303.
[14] R.C. Young, R.C. Mitchell, T.H. Brown, C.R. Ganellin, R. Griffiths, M. Jones, K.K. Rana, D. Saunders, I.R. Smith, N.E. Sore, T.J. Wilks, Development of a new physicochemical model for brain penetration and its application to the design of centrally acting H2 receptor histamine antagonists, J. Med. Chem. 31 (1988) 656–671.
[15] J.M. Luco, Prediction of the blain–blood distribution of a large set of drugs from structurally derived descriptors using partial least-squares (PLS) modeling, J. Chem. Inf. Comput. Sci. 39 (1999) 396–404.
[16] D.E. Clark, Rapid calculation of polar molecular surface area and its application to the prediction of transport phenomena: 2. Prediction of blood–brain barrier penetration, J. Pharm. Sci. 88 (1999) 815–921.
[17] J. Kelder, P.D.J. Grootenhuis, D.M. Bayada, L.P.C. Delbressine, J.P. Ploemen, Polar molecular surface as a dominating determinant for oral absorption and brain penetration of drugs, Pharm. Res. 16 (1999) 1514–1519.
[18] P. Ertl, B. Rohde, P. Selzer, Fast contribution of molecular polar surface area as a sum of fragment-based contributions and its application to the prediction of drug transport, J. Med. Chem. 43 (2000) 3714–3717.
[19] M. Feher, E. Sourial, J.M. Schmidt, A simple model for the prediction of blood–brain partitioning, Int. J. Pharm. 201 (2000) 239–247.
[20] U. Norinder, P. Sjoberg, T. Osterberg, Theoretical calculation and prediction of brain–blood partitioning of organic solutes using MolSurf parameterization and PLS statistics, J. Pharm. Sci. 87 (1998) 952–959.
[21] G. Cruciani, P. Crivori, P.A. Carrupt, B. Testa, Molecular fields in quantitative structure permeation relationships: the VolSurf approach, J. Mol. Struct., Theochem 503 (2000) 17–30.
[22] L.H. Alifrangis, I.T. Christensen, A. Berglund, M. Sandberg, L. Hovgaard, S. Frokjaer, Structure–property model for membrane partitioning of oligopeptides, J. Med. Chem. 43 (2000) 103–113.
[23] P. Crivori, G. Cruciani, P.A. Carrupt, B. Testa, Predicting blood–brain barrier permeation from three-dimensional molecular structure, J. Med. Chem. 43 (2000) 2204–2216.
[24] J.H. Lin, I.W. Chen, T.H. Lin, Blood–brain barrier permeability and in vivo activity of partial agonists of benzodiazepine receptor: a study of L-663,581 and its metabolites in rats, J. Pharmacol. Exp. Ther. 271 (1994) 1197–1202.
[25] T. Salminen, A. Pulli, J. Taskinen, Relationship between immobilised artificial membrane chromatographic retention and the brain penetration of structurally diverse drugs, J. Pharm. Biomed. Anal. 15 (1997) 469–477.
[26] M.H. Abraham, H.S. Chadha, R.C. Mitchell, Hydrogen bonding: 33. Factors that influence the distribution of solutes between blood and brain, J. Pharm. Sci. 83 (1994) 1257–1268.
[27] SYBYL 6.4, Tripos Associates, St. Louis, MO, 1995.
[28] P.J. Goodford, A computational procedure for determining energetically favorable binding sites on biologically important macromolecules, J. Med. Chem. 28 (1985) 849–857.